Annals of Biomedical Engineering, Vol. 20, pp. 149–165, 1992
Printed in the USA.

0090-6964/92 $5.00 + .00

A Conical Model to Describe the Nonuniformity of the Left Ventricular Twisting Motion

H. Azhari,* M. Buchalter,† S. Sideman,* E. Shapiro,† and R. Beyar*

*The Heart System Research Center
Julius Silver Institute
Department of Biomedical Engineering
Technion – Israel Institute of Technology
Haifa 32000, Israel

†Division of Cardiology
Johns Hopkins Medical Institutions
Baltimore, MD

(Received 6/21/90; Revised 4/22/91)

The systolic contraction and fiber shortening in the left ventricle (LV) produces torsional moments in the myocardium, resulting in a gradient of angular displacements about the long axis. This is manifested as a counterclockwise rotation of the apex relative to the base, when viewed from the apex. Recent studies with magnetic resonance imaging (MRI), using noninvasive magnetic tags, have revealed three important properties of the LV twist: (a) The angle of twist (i.e., the angular rotation of a slice relative to the basal slice) is consistently higher at the endocardium as compared to the epicardium; (b) The twist increases towards the apex; and (c) Straight MRI-tagged radial lines at end-diastole (ED) are slightly curved at end-systole (ES), implying a nonlinear transmural variation of the twist. The present study suggests that the geometry of the LV at ES can be represented by a thick-walled hollow cone, and that the transmural twist patterns from ED to ES can be described using the continuum mechanics approach and a small strain analysis of an isotropic cone subjected to external torque. The predicted results are compared with the noninvasive MRI measurements of transmural twist in eight human volunteers. Given the epicardial angles of twist of each slice, the predicted endocardial angles of twist are in good correlation with the experimental findings ($r = 0.86$, slope $= 1.09$, SEE $= 4.1°$). In addition, the model reliably describes the changes in the twist magnitude from apex to base (no significant difference from experimental values, $P = 0.2$), and predicts the curvilinear pattern at ES of the originally straight ED radial lines. Thus, the conical model with uniform properties of the LV, reliably predicts the nonuniformity of the twist patterns, implying that the LV twist is strongly affected by LV geometry.

Keywords—*Left ventricle, Model, Cone, Twist, Nonuniformity.*

Acknowledgments—This study was supported in part by the Edythe and Joseph Jackier Foundation, American Technion Society, Detroit, United States; the Adelaide and Michael Kennedy Leigh Endowment Fund, London, United Kingdom; and by the Israel-U.S. Binational Science Foundation, Grant No. 84-00380.

Address correspondence to R. Beyar, M.D., D.Sc., Department of Biomedical Engineering, Technion-IIT, Haifa, 32000, Israel.

INTRODUCTION

The twisting motion of the left ventricle (LV), defined as the gradient of angular displacement of a myocardial point around the long axis, is an important physiological phenomenon, which is closely associated with torsional deformation, and the transmural fiber shortening and stresses. Various models have been proposed to explain the forces responsible for this deformation and its consequences on the transmural fiber shortening (2,5,6,9). To date, the degree of twist of the endocardium (defined here as angular rotation relative to the base of the heart) has been measured by echocardiography (1); that of the midwall by using multiple implanted markers (7,11,12,14), and that of the epicardium by using either metal (17) or surface markers (3). However, most of these local measurements were not obtained simultaneously, or were based on invasive procedures, which may have affected the myocardium or could not be applied to the septal wall. As a result, little is known about the transmural characteristics of the LV twist and its variation from one LV site to the other. This is particularly true for the *in vivo* human heart. Consequently, attempts to calculate and analyze the twisting motion have usually been based on the assumption that there are no transmural differences in the twisting angle (2,5,6,9); that is, that the torsional deformation of the LV occurs without circumferential transmural shear (θr plane in a cylindrical coordinate system $rz\theta$). However, measurements with transmurally implanted markers have suggested the existence of transmural shear and Waldman, Fung, and Covell (27) have demonstrated the existence of both circumferential transmural (θr), and longitudinal transmural (zr) shear strains. Furthermore, the novel new noninvasive magnetic resonance imaging (MRI)-based measurement method, using MR-excited straight cross-sectional tag lines (30), which are "imprinted" on the LV image at end-diastole (ED) and then measured on the end-systole (ES) images, have conclusively shown that the magnitude of the endocardial twist is significantly higher than the epicardial twist (8). The curved MRI tag lines observed at ES represent the effect of transmural circumferential shear, which is clearly a function of the radial distance from the endocardium. These recent findings can be attributed to the characteristic fibrous structure of the myocardium, or to the geometry of the LV, or to both.

Many previous models (2,10,19,23,24,26) have chosen to focus on the fibrous structure (22) while approximating the LV geometry by a cylindrical shape. However, while some (13) have included the transverse circumferential shear, these cylindrical models do not account for the longitudinal variation of torsional shear. Furthermore, the epicardial moments in the cylindrical model dominate (and the twist occurs in the direction of the epicardial moments), while the endocardial moments oppose the twisting motion of the LV. Consequently, it is to be expected that the epicardial twist of the tightly tethered structure of the myocardium will be higher, or at least equal, to the endocardial twist in the cylindrical model (see Appendix A). However, this is contrary to the reported MRI measurements (8).

In view of the above disagreement between observation and theory, it is reasonable to expect that the shape of the LV may play an important role in the analysis of the transmural twist pattern. Here, we suggest a model for describing the LV deformation patterns associated with twist, which is primarily based on a conical geometry. The deformation in this model is calculated assuming that the moments, which are generated by its fibrous structure, can be represented by external moments applied

to a geometrically equivalent hollow cone with a constant shear modulus. The calculated results are consistent with the reported experimental finding of a higher endocardial than epicardial twist, with the observed base to apex increase of angular displacement, and with the curvilinearity of the transmural twist, especially towards the apex.

METHODS

Measurement of the Twist by Tagged MR Images

The experimental data were acquired in a study which is described in detail elsewhere (8), and only a brief description of the experimental procedure is given here. Eight normal human volunteers (5 male and 3 female, age 24–38) were imaged in a 0.38T iron core, resistive magnet (Resonnex RX4000). After several scout scans, the image planes were positioned so that the obtained short-axis, cross-sectional images were perpendicular to the long axis of the LV. Five equally spaced parallel short-axis images, from base to apex, were tagged at ED (gated by the ECG signal) and aquired at ES (timed to the first high frequency component of the second heart sound, S2, as determined by phonocardiography). The MRI tagging, explained in detail elsewhere (30), is produced by activating four equiangular, radial presaturation planes; this results in each tomographic slice being marked by eight equally spaced straight radial tag lines at ED (Fig. 1). The intersections of these tag lines with the endocardial (eight points) and epicardial borders (eight points) are traced and the angle of ES twist calculated from the rotation of each of the endocardial and epicardial points relative to the basal image (8). The angles of twist of an epicardial or an endocardial contour reported herein for each slice represent the average twist values of these eight epicardial or endocardial points relative to the basal image, respectively.

General Approach and Basic Assumptions

It is suggested here that the LV geometry governs the nonuniformity of the twist patterns. To substantiate this assumption, we demonstrate that twisting a cone with a geometry similar to that of the LV, and with homogeneous elastic properties matched to the LV properties; yields patterns of twist displacements similar to those actually measured for the LV. For simplicity, the strain analysis is carried out using "small strain" theory. The estimated error resulting from this approximation is outlined in Appendix B, where a comparison to a "finite strain" approach is carried out. The method of extracting the elastic properties required for the model from the experimental data is explained below. To justify the use of uniform properties, the analysis is first applied to one slice at a time. Then, the complete conical model of average geometrical and elastic properties is used to obtain the typical twist patterns for the entire LV.

Conical Approximation of the LV Geometry

The LV geometry is characterized by a gradual decrease, from base to apex, of the endocardial and epicardial diameters and the myocardial thickness (21). These characteristics may be approximated by describing the ventricular geometry by a hollow conical shell (Fig. 2). Clearly, the conical shape is a better approximation of the actual

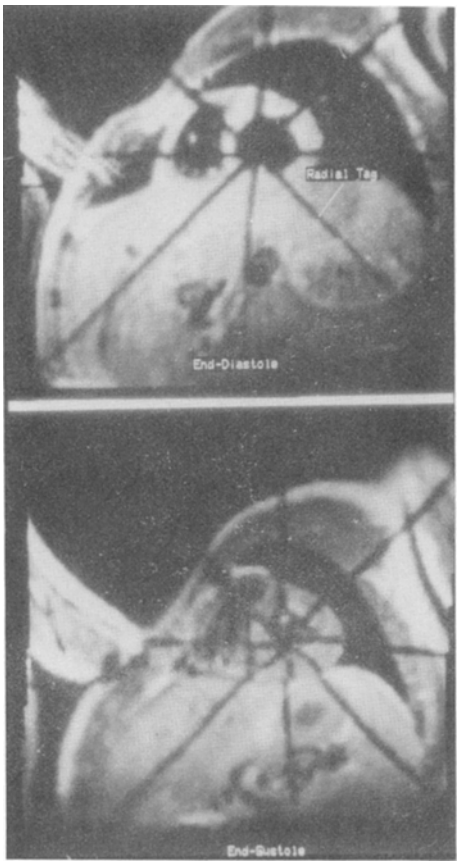

FIGURE 1. A typical tagged MRI image of a LV. Note the straight tag lines at ED (top) and their deformed state at ES (bottom).

LV geometry than a cylinder, which obviously does not account for the base-to-apex decrease in both the diameter and wall thickness. The epicardial surface is described here by a cone of angle α while the endocardial surface is described by a cone of angle β, with a common apex at the axes origin 0. A least-squares linear regression analysis was used to obtain the point of origin 0 and the endocardial and epicardial angles of each individual LV. First, regression analysis was applied separately for the endocardial and epicardial radii R versus the distance Z' from the LV base, yielding a line $R = aZ' + b$. Then the corresponding conical angle was calculated from $\alpha = \arctan(a)$, and the cone's apex was taken at $Z_0 = -b/a$ for the endocardium and epicardium. Since the calculated line was not constrained to pass through the anatomical apex, taken as one interslice distance below the last available cross section, each surface (endocardium and epicardium) yielded its own apex. The common geometrical apex (point 0) was then taken as the average between the endocardial and epicardial values of Z_0.

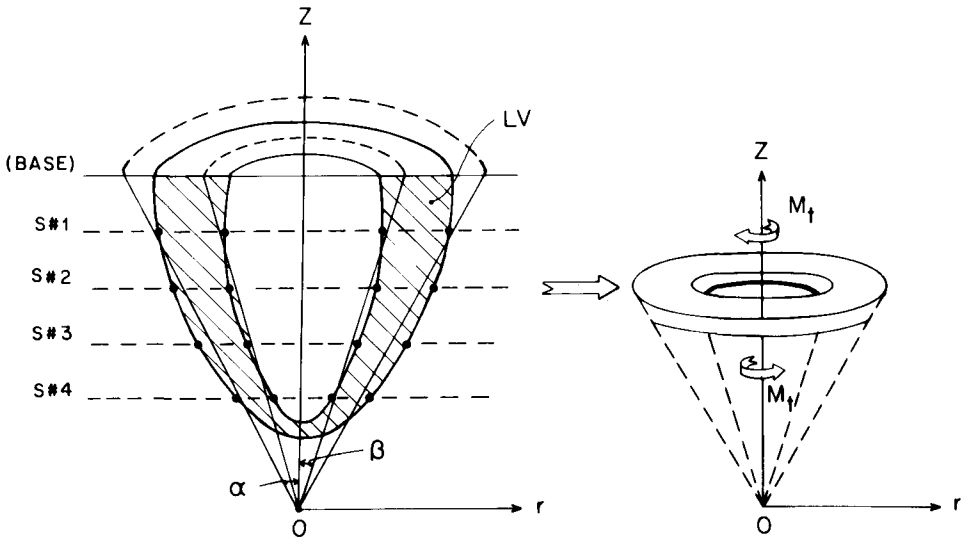

FIGURE 2. A schematic depiction of the hollow conical geometry utilized here to approximate the LV. (α and β are the epicardial and endocardial cone angles, respectively, M_t is the applied moment, *S#n* is the measured tomographic slice number *n*.) Note that the cone's apex 0 does not align with the anatomical apex.

Stress and Angle of Twist

From the theory of elasticity (25), the stress function $\Phi = \Phi(r,z)$ of a circular shaft, with a variable diameter subjected to a twisting moment, fulfills the following differential equation:

$$\partial^2\Phi/\partial r^2 - 3\partial\Phi/r\partial r + \partial^2\Phi/\partial z^2 = 0 \ , \tag{1}$$

with the boundary condition given by:

$$(\partial\Phi/\partial z)\cdot(\partial z/\partial s) + (\partial\Phi/\partial r)\cdot(dr/\partial s) = 0 \ , \tag{2}$$

where ds is an element of the boundary. It follows from Eq. 2 that Φ is constant along the boundary of the axial section of the shaft. The relation between the applied twisting moment M_t and Φ is determined from the following equilibrium equation:

$$M_t = -2\pi \int_{R_{in}}^{R_{out}} (\partial\Phi/\partial r)\, dr = -2\pi \left| \Phi \right|_{R_{in}}^{R_{out}} \ , \tag{3}$$

where R_{in} is the radius of the inner surface and R_{out} is the radius of the outer surface.

The relation between the stress function and the angle of twist $\psi = \psi(r,z)$ is given by (25):

$$G \cdot (\partial \psi / \partial r) = -1/r^3 \partial \Phi / \partial z \tag{4a}$$

$$G \cdot (\partial \psi / \partial y) = -1/r^3 \partial \Phi / \partial r \ , \tag{4b}$$

where G, the shear modulus of elasticity, is assumed here to be constant.

Considering the conical geometry of the LV, and taking the coordinate origin at 0, it is seen that

$$Z/(R^2 + Z^2)^{1/2} = \left\{ \begin{matrix} \cos(\alpha) \text{ @ epicardium} \\ \cos(\beta) \text{ @ endocardium} \end{matrix} \right\} = \text{constant} \ , \tag{5}$$

that is, the ratio in Eq. 5 is constant at the boundaries. Any function of this ratio will therefore readily fulfill the boundary condition, Eq. 2.

To satisfy Eq. 1, the stress function Φ can take the following form (25):

$$\Phi = C\{z/(r^2 + z^2)^{1/2} - 1/3[z/(r^2 + z^2)^{1/2}]^3\} \ , \tag{6}$$

where C is a constant. Substituting Eq. 6 into Eq. 3 and utilizing Eq. 5 yields the value of C:

$$C = -M_t/2\pi[(\cos\alpha - \cos\beta) + 1/3(\cos^3\beta - \cos^3\alpha)] \ . \tag{7}$$

Substituting Φ into Eqs. 4a and 4b and solving for ψ yields:

$$\psi(r,z) = -M_t/6\pi G[(\cos\alpha - \cos\beta) + 1/3(\cos^3\beta - \cos^3\alpha)]\,(r^2 + z^2)^{3/2} \tag{8}$$

Note that in the human heart, twist occurs in the counterclockwise direction as observed from the LV apex; that is, the apex rotates counterclockwise relative to the base when viewed from the apex. Thus, ψ is taken here to be positive in that direction.

Boundary Conditions and Material Properties

Equation 8 provides the relation between the applied torque M_t and the angle of twist ψ. However, the values of both M_t and G are unknown, as both are determined by the unknown instantaneous state of the activated myocardial fibers. On the other hand, the angles of twist at the endocardial and epicardial boundaries of each studied slice are known from the experimental measurements, and the ratio M_t/G can thus be determined for each slice. Hence, the following procedure was adopted here. Each slice was assumed to be isolated from the rest of the LV and be part of a conical shaft which has constant values of M_t and G (Fig. 2b). The ratio of M_t/G was then determined from the measured angle of twist at the epicardium, and the corresponding endocardial angle of twist calculated by Eq. 8 for each slice. The M_t/G values obtained from all hearts for slices of equal height were averaged and used to determine if and how the M/G ratio varies from apex to base. The typical twisting patterns were then calculated from the given average values of M_t/G.

Statistical Analysis

Standard linear regression was used to evaluate the correlation between the measured and calculated endocardial twist of each slice. The Friedman nonparametric test

was used to check for a difference between levels in the M_t/G ratio. Two-way analysis of variance was used to test for similarity between measured and model prediction results for the different levels of the LV ($p < 0.05$ was assumed to be the level of significance).

RESULTS

Geometrical Data

As shown schematically in Fig. 2, the geometry of each of the 8 LVs was approximated using a hollow conical shaft configuration. The epicardial (α) and endocardial (β) inclination angles to the long axis of the LV, as well as the distance Z_0 of the geometrical apex (point 0 in Fig. 2) from the LV base, were determined by using linear regression analysis on the measured $R(Z')$ values as detailed above. The results are summarized in Table 1.

The results indicate that the conical geometrical approximation at ES is rather satisfactory. The correlation coefficients, ρ, for the endocardial and epicardial surfaces were relatively high ($\rho = 0.82 \pm 0.04$ and $\rho = 0.89 \pm 0.04$ for the epicardial and endocardial surfaces, respectively). Also, the scatter of the cone's angles was relatively small ($\alpha = 27.9° \pm 1.8$ and $\beta = 16.5° \pm 0.8$). The conical approximation is further supported by the finding that the individually calculated locations of the geometrical apex for the endocardial and epicardial surfaces (Z_{01} and Z_{02}) did not differ by more than 0.9 cm (average = 0.6 ± 0.3 cm).

Calculated versus Measured Endocardial Angle of Twist

Using the geometrical parameters α, β, and Z_0, obtained for each LV, the epicardial angle of twist at each measured point was used, along with its (r, z) coordinate, as input for each slice and, by Eq. 8, utilized to estimate the M_t/G ratio for that par-

TABLE 1. Average geometrical values obtained by approximating the left ventricle by a conical geometry. Data was acquired *in vivo* from eight human subjects by MRI tagging.

	Epicardium			Endocardium			Common	
Case #	α	Z_{01}	ρ	β	Z_{02}	ρ	$\lvert Z_{01} - Z_{02} \rvert$	Z_0
1	26.9	−8.9	0.74	16.7	−8.0	0.85	0.9	−8.4
2	26.6	−9.7	0.81	16.7	−9.3	0.85	0.4	−9.5
3	29.5	−7.7	0.81	17.1	−7.1	0.91	0.6	−7.4
4	25.6	−9.1	0.87	15.6	−8.6	0.93	0.5	−8.9
5	31.3	−8.4	0.87	17.9	−8.2	0.83	0.2	−8.3
6	27.5	−9.6	0.82	16.3	−8.7	0.93	0.9	−9.2
7	27.2	−9.6	0.82	16.3	−8.7	0.93	0.9	−9.1
8	28.3	−8.1	0.84	15.5	−7.6	0.92	0.5	−7.8
Average	27.9		0.82	16.5		0.89	0.6	−8.6
±*S.D.*	±1.8		±0.04	±0.8		±0.04	±0.3	±0.7

α, β = cone angles of the endocardium and epicardium, respectively; Z = height of slice from the geometrical apex, cm; Z_0 = distance of geometrical apex from LV base, cm; ρ = correlation for radius versus height regression line.

TABLE 2. Average of measured epicardial twist ψ_0, r, and z coordinates of the endocardium, M_t/G ratio, as well as calculated and measured angles of twist ψ at the endocardium at four different levels of the left ventricle.

Slice #	ψ_0 (Epi)	Z (cm)	r (cm)	M_t/G (cm^3)	Measured ψ (Endo)	Predicted ψ (Endo)
Base 1	2.0° ± 0.5	7.2 ± 0.6	1.8 ± 0.2	3.34 ± 2.40	4.4° ± 1.9	2.3° ± 1.7
2	3.7° ± 0.8	5.8 ± 0.5	1.6 ± 0.2	3.62 ± 1.30	7.4° ± 2.2	4.7° ± 1.9
3	7.1° ± 0.8	4.4 ± 0.4	1.4 ± 0.2	3.81 ± 1.76	13.4° ± 2.5	9.8° ± 2.5
Apex 4	11.2° ± 1.0	3.0 ± 0.3	1.2 ± 0.2	2.82 ± 1.02	18.9° ± 3.2	21.5° ± 3.2

M_t = applied twisting moment; G = modulus of elasticity in shear for the LV.

ticular slice. The endocardial angle of twist was then determined by Eq. 8, using the calculated M_t/G ratio and the given r, z coordinates for the measured endocardial point. The calculated results are summarized in Table 2 and compared in Fig. 3. As can be noted, there are little variations in M_t/G from base to apex, and the Friedman nonparametric test showed no overall difference in M_t/G between the levels ($p = NS$). This finding implies that a single M_t/G value can be utilized to describe the twist pattern of the entire LV.

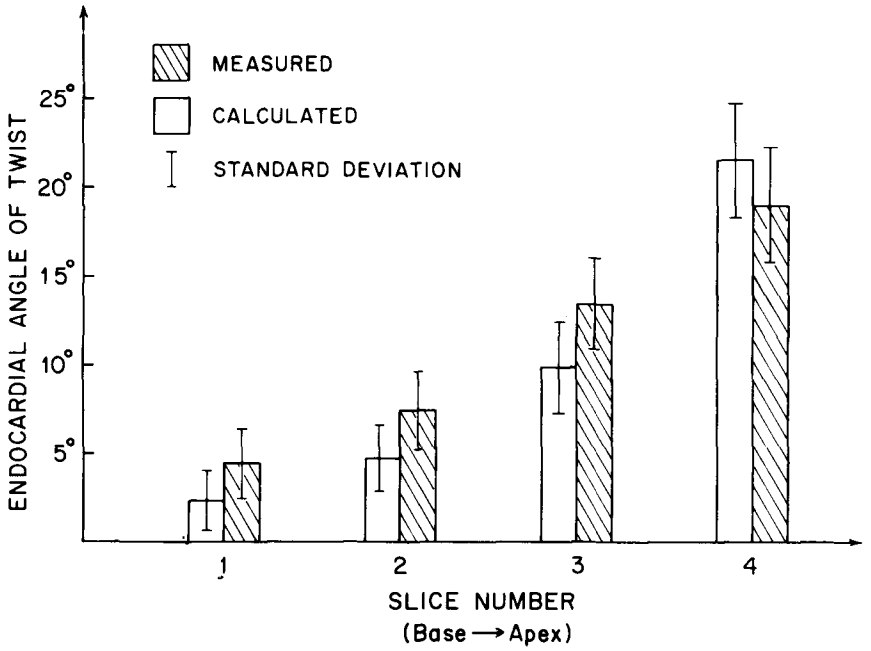

FIGURE 3. Comparison of the averaged predicted endocardial angles of twist to the measured angles of twist by MRI tagging, obtained from eight human LVs studied *in vivo*. Note the fair agreement between the theoretical and experimental values.

Furthermore, analysis of variance comparing the measured and the predicted values of the endocardial twist showed no overall difference between them ($p = 0.2$). Comparing the calculated angle of twist for each point studied at the endocardium (y) to its corresponding measured value (x) (Fig. 4), and applying a linear regression analysis, yielded a regression line $y = 1.09x - 2.43°$ ($r = 0.86$, $SEE = 4.1°$), thus validating the predictive power of the suggested model.

Twisting Patterns

Longitudinal Changes. As noted above, the calculated M_t/G ratios outlined in Table 2 are fairly constant (though with a very large scatter). Thus, Eq. 8 can be applied without modification to predict the twisting patterns throughout the LV. The calculated average M_t/G ratio (= 3.4) and the average cone angles of $\alpha = 27.9°$ and $\beta = 16.5°$, were used to calculate the endocardial and epicardial angles of twist from the LV base to apex, depicted in Fig. 5. As can be observed, the angle of twist increases exponentially from the LV base toward the apex. It can also be observed that the epicardial angle of twist is consistently smaller than the endocardial one, with the gap between the two increasing towards the apex. These patterns are in good agreement with the reported experimental findings (8).

Radial Changes. As experimentally observed (8), the radial straight MR tag line "impressed" at ED depicts a relatively parallel displacement at ES, resulting from the

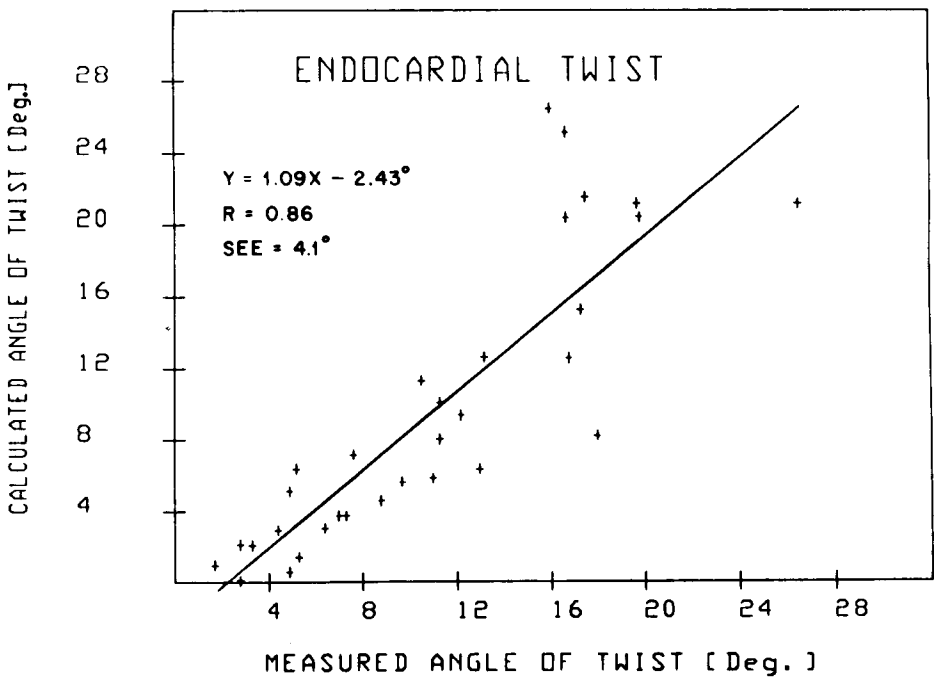

FIGURE 4. A point-to-point comparison between the measured angles of endocardial twist and the calculated ones. Data corresponds to 32 points (4 slices × 8 hearts).

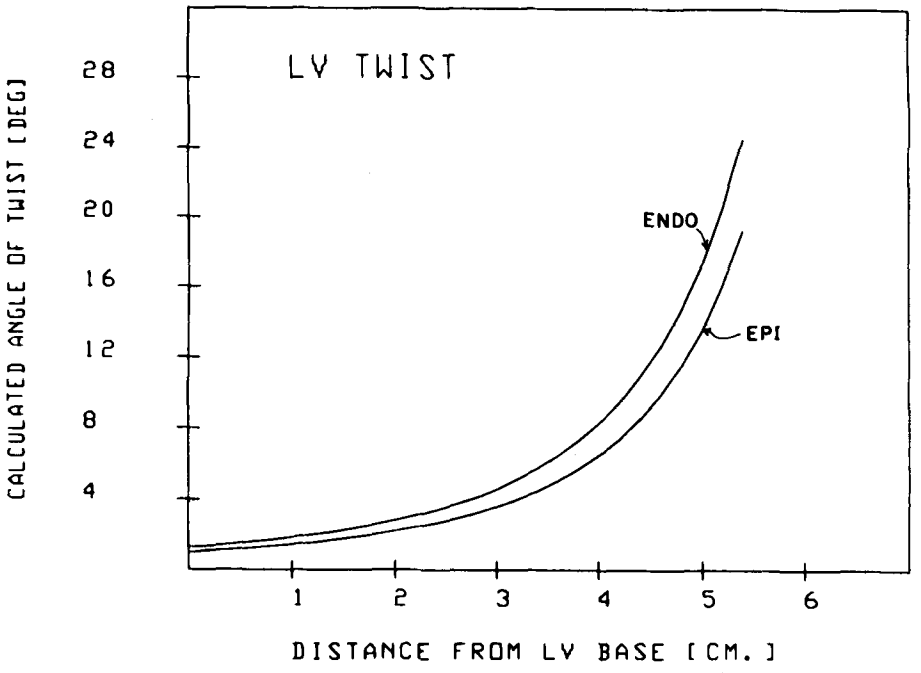

FIGURE 5. Model prediction of the endocardial and epicardial angles of twist from LV base towards the apex. Note the consistently higher endocardial angle of twist with respect to the epicardial one and the increasing gradient between the two.

larger endocardial twist. Furthermore, the straight tag lines at ED are observed to be slightly curved at ES (Fig. 1b), especially at the apical zone.

The predicted location, at ES, of the originally (at ED) straight tag line is depicted in Fig. 6a. The pattern of the transmural deformation is consistent with the experimental MRI data (8), showing higher endocardial than epicardial twist. Moreover, the ES deformation of each point along a horizontal radial tag line, plotted in greater detail in Fig. 6b for an apical slice, shows the typical curvilinearity observed in the MRI measurements. These results further demonstrate the agreement between the model's predictions and the reported experimental findings (e.g., Fig. 1).

Lines of Equal Twist. It is interesting at this point to investigate the "iso-twist" surfaces; that is, the locations that have the same angle of twist. Introducing a constant value of ψ in Eq. 8, it can easily be shown that the constraint for (r,z) is:

$$r^2 + z^2 = \text{constant} \ . \tag{9}$$

This relation implies that all the lines of the same angle of twist in the r, z plane are located along circles whose centers are at point 0 (Fig. 7). Thus, as the system is symmetric with respect to θ, the "iso-twist" surfaces are actually concentric spheres, which center is at point 0.

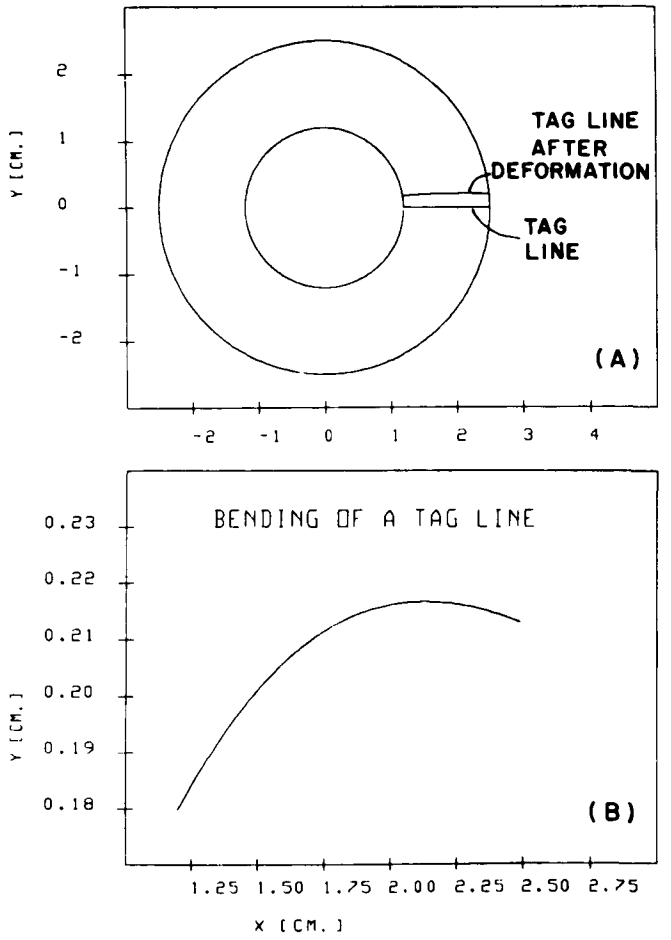

FIGURE 6. (a) Model prediction of the deformation of a straight radial tag line due to LV twist; (b) A detailed view of the deformed tag line depicted in (a). Note the predicted bending of the initially horizontal tag line.

DISCUSSION

The phenomenon of LV torsional deformation, or twist, is well documented in the literature. Qualitative experimental observations of this phenomenon were already reported in 1669 by Richard Lower (15). More recent experimental reports (3,7,11,12,14) have provided quantitative values of the twist. However, attempts to predict the angle of twist via analytical models have mostly focused on the fibrous structure of the LV, while neglecting the role of the LV geometry, and usually approximating it by a cylinder (2,10,19,24,26). Furthermore, most past models have neglected transmural changes in the angle of twist; an assumption that is contradictory to the recently reported experimental findings of a gradient in the amount of twist across the LV wall (8).

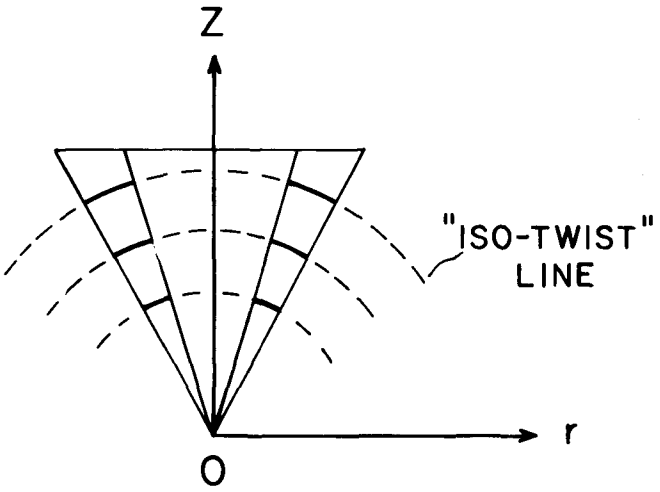

FIGURE 7. Theoretical prediction of the "iso-twist" lines. Note that all such lines are located in the *r–z* plane along concentric circles, which center is at point 0.

The present study demonstrates that the nonuniformity of the longitudinal and transmural twist patterns can be reliably predicted by employing a model that approximates the LV by a hollow cone of uniform material properties. The model emphasizes the role of the LV geometry and assumes that the internally generated moments, which stem from the helical structure of the myocardial fibers, can be represented by externally applied moments, which cause the torsional deformation of the LV myocardium. The proposed model predicts the experimentally determined transmural twist gradient, with the endocardial twist angle exceeding the epicardial one, and shows that this gradient increases from the LV base towards the apex (Fig. 5). Good quantitative agreement was also found between the theoretical predictions of the endocardial twist angles and the experimentally reported ones ($R = 0.86$, using linear regression analysis), and between the theoretical and experimental overall variation of these angles from the LV base to apex ($p = 0.2$, indicating no significant difference, using two-way analysis of variance). It also demonstrates the ED-to-ES curvilinear deformation of straight tag lines across the LV wall (Fig. 6). Given that homogeneous material properties were used here, these results imply that LV geometry alone may play a major role in the genesis of the LV transmural twist gradient.

Though inaccurate, the use of homogeneous material properties to model the LV helps elucidate some characteristics of the twist phenomena. Homogeneous models by Mirsky (18) and Wong and Rautaharju (29) have contributed to our understanding of the mechanical function of the LV. Indeed, considering the fibrous structure of the LV as described by Streeter *et al.* (22), one may expect a significant heterogeneity of the material properties and the LV mechanical function across the LV wall. However, the ability of homogeneous models with the proper geometry, such as the one presented here, to reliably predict certain properties of transmural myocardial deformation imply the the LV deforms as a highly tethered structure once the torsional moments are generated by the fibrous structure of the myocardium. This conclusion

is supported by other experimental findings such as those of Waldman *et al.* (28), who have shown that the transmural variation in the direction of the principal strains within the myocardial layers is significantly smaller than the corresponding variation in fiber orientation; a phenomena which may be attributed to the interlayer tethering. Also, the reports of Rademakers *et al.* (20) have shown that cross-fiber deformation in the endocardium exceeds the deformation along the fibers, a phenomena which may be attributed to the geometrical coupling of the myocardial layers. Clearly, the LV geometry is an important parameter in the transmural twisting pattern, and depending on the theoretical approach taken, plays a relatively more important role than the inhomogeneity and anisotropy of the myocardium.

In the present study, emphasis is put on the effect of the LV shape on the transmural and longitudinal nonuniformity of the twisting motion. While it is important to eventually relate this displacement to the myocardial fibrous structure, it is noteworthy that the role of this structure is presently implicitly incorporated in the model through the M_t/G ratio in Eq. 8. M_t, the torsional moment, may be considered as the resultant of the opposing transmural moments acting within the LV walls, due to the transmurally varying inclination angle of the fibers (from $+60°$ to $-60°$ from endocardium to epicardium (22)). Similarly, G, the shear modulus, may be viewed as the amount of tethering between the fibers. Interestingly and not surprisingly, the results obtained here indicate that the ratio M_t/G is relatively constant from apex to base (Table 2). This may be interpreted in two alternative ways: (a) Both M_t and G remain constant throughout the LV; (b) Both change proportionally between levels. However, this issue cannot be resolved with the currently available data.

The approximation of the LV shape by a conical geometry is further substantiated by the linear regression results in Table 1 ($\rho = 0.89$ for the endocardium and $\rho = 0.82$ for the epicardium). Obviously, the cone is better than the cylinder as an approximation to the ES LV shape. This approximation may appear to be somewhat at odds with the commonly accepted geometrical model of a truncated ellipsoid suggested by Streeter and Hanna (21), and many others (18,29). However, it is interesting to note that the ellipsoidal description of the LV was usually derived from *in vitro* or open chest studies, mostly of dogs. The current study, on the other hand, is based on noninvasive *in vivo* studies of intact human hearts. Furthermore, 3-D computer reconstructions of the LV, obtained from *in vivo* scans from healthy human subjects (4), demonstrate that under normal conditions the LV shape has conical characteristics at ES.

It is noteworthy that fibrous cylindrical models, which account for myocardial fiber mechanics in great detail (e.g., 2,10,19,22), successfully predict the average global LV twist, but do not account for transmural variation effects due to longitudinal changes in the LV geometry. In fact, as shown in the Appendix, the fibrous models with cylindrical geometry should result in a transmural twist gradient, which is inconsistent with the observed experimental gradients. As demonstrated in this study, the LV geometry is a critical factor in the manifestation of the twist phenomena. Clearly, incorporation of the fibrous myocardial structure of the LV in the proper geometrical model should greatly help to elucidate the phenomena of the global and transmural twist deformation of the LV. Furthermore, an isotropic LV model, which is subjected to external moments, may not be the correct physical characterization of the twisting LV. It is possible that a more realistic model using internally generated twist moments may lead to different results and conclusions. The main point taken by this work is to emphasize the importance of shape on the twist deformation. There-

fore, while the current model may use oversimplified material properties of the myocardium, it clearly shows that the LV geometry may be the dominant factor in determining the transmural twist gradient. Future models, which will be able to incorporate internal moments with material anisotropy to describe the transmural shears, should take into account the geometry of the LV, particularly towards the apex.

Another limiting point to be considered is the use of the small deformation analysis. However, as shown in Appendix B, this assumption introduces a relatively small error in the analysis and does not affect the major conclusion regarding the important effect of the conical geometry on the twist characteristics.

Summary

A model that predicts the transmural twist patterns of the LV has been introduced. The model approximates the LV by a hollow cone with homogeneous material properties. The model predicts the transmural patterns of twist and the longitudinal variation of the twist, which are similar to the experimental data obtained by MRI tagging. The model emphasizes the dominant role of the geometry of the LV on the transmural and longitudinal LV twist patterns.

REFERENCES

1. Arts, T.; Meerbaum, S.; Reneman, R.S.; Corday E. Torsion of the left ventricle during the ejection phase in the intact dog. Cardiovasc. Res. 18:183–193; 1984.
2. Arts, T.; Reneman, T.S.; Veenstra P.C. A model of the mechanics of the left ventricle. Ann. Biomed. Eng. 7:299–318; 1979.
3. Arts, T.; Veenstra, P.C.; Reneman, R.S. Epicardial deformation and left ventricular wall mechanics during ejection in the dog. Am. J. Physiol. 243 (Heart Circ. Physiol. 12):H379–H390; 1982.
4. Azhari, H.; Grenadier, E.; Dinnar, U.; Beyar, R.; Adam, D.; Marcus, M.L.; Sideman, S. Quantitative characterization and sorting of three dimensional geometries: Application to left ventricles *in vivo*. IEEE Trans. Biomed. Eng. 36:322–332; 1989.
5. Beyar, R.; Sideman, S. A computer study of left ventricular performance based on fiber structure, sarcomere dynamics, and transmural electrical propagation velocity. Circ. Res. 55:358–375; 1984.
6. Beyar, R.; Sideman, S. The dynamic twisting of the left ventricle. Ann. Biomed. Eng. 14:547–562; 1986.
7. Beyar, R.; Yin, F.; Hausknecht, M.; Weisfeldt, M.L.; Kass, D. Dependency of Left ventricular twist shortening relationship on cardiac cycle phase. Am. J. Physiol. 257 (Heart. Circ. Physiol. 26):H119–H1126; 1989.
8. Buchalter, M.B.; Weiss, J.L.; Rogers, W.J.; Zerhouni, E.A.; Weisfeldt, M.L.; Beyar, R.; Shapiro, E.P. Non-invasive quantification of left ventricular rotational deformation in normal humans using magnetic resonance imaging myocardial tagging. Circulation 81:1236–1244; 1990.
9. Chadwick, R.S. Mechanics of the left ventricle. Biophys. J. 39:279–288; 1982.
10. Guccione, J.M.; McCulloch, A.D.; Waldman, L.K. Passive material properties of intact ventricular myocardium determined from a cylindrical model. Trans. of the ASME 113:42–55; 1991.
11. Hansen, D.E.; Daughters, G.T.; Alderman, E.L.; Ingels, N.B.; Miller, D.C. Torsional deformation of left ventricular midwall in human hearts with intramyocardial markers: Regional heterogeneity and sensitivity to inotropic effect of abrupt rate changes. Circ. Res. 62:941–952; 1988.
12. Hansen, D.E.; Daughters, G.T.; Alderman, E.L.; Stinson, E.B.; Baldwin, L.C.; Miller, D.C. Effects of acute human cardiac allograft rejection on left ventricular systolic torsion and diastolic recoil measured by intramyocardial markers. Circulation 5:998–1008; 1987.
13. Humphrey, J.D.; Yin, F.C.P. On constitutive relations and finite deformations of passive cardiac tissue II: Stress analysis in the left ventricle. Circ. Res. 65:805–817; 1989.
14. Ingels, N.B.; Daughters, G.T.; Stinson, E.B.; Alderman, E.L. Measurements of midwall myocardial dynamics in intact man by radiography of surgically implanted markers. Circulation 52:859–867; 1975.
15. Lower, R. Tractus de corde. In: Early science in Oxford; Vol. 9. Oxford, UK: RT Gunther; 1932. London: Swansons, Pall Mall Reprint; 1968.

16. Malvern, L.D. Introduction to the Mechanics of a continuous medium. Englewood Cliffs, NJ: Prentice-Hall, Inc.; 1969.
17. McDonald, I.G. The shape and movements of the human left ventricle during systole: A study by cine-angiography and by cineradiography of epicardial markers. Am. J. Cardiol. 26:221–237; 1970.
18. Mirsky, I. Left ventricular stresses in the intact human heart. Biophys. J. 9:189–208; 1969.
19. Nevo, E.; Lanir, Y. Structural finite deformation model of the left ventricle during diastole and systole. Trans. ASME: J. Biomech. Eng. 111:342–349; 1989.
20. Rademakers, F.E.; Rogers, W.J.; Meils, C.M.; Buchalter, M.B.; Bush, D.E.; Guier, W.H.; Weisfeldt, M.L.; Weiss, J.L.; Shapiro, E.Pl. Extensive myocardial shortening occurs perpendicular to fiber orientation: Transmural and regional variation. Circulation 82(4)[Supp. III-172]:Abstract-0682; 1990.
21. Streeter, D.D., Jr.; Hanna, W.T. Engineering mechanics for successive states in canine left ventricular myocardium: I. Cavity and wall geometry. Circ. Res. 33:639–655; 1973.
22. Streeter, D.D.; Spotnitz, H.M.; Patel, D.P.; Ross, J.; Sonnenblick, E.H. Fiber orientation in the canine left ventricle during diastole and systole. Circ. Res. 24:339–347; 1969.
23. Taber, L.A. On a nonlinear theory for muscle shells: Part I—Theoretical development. Trans. of the ASME 113:56–62; 1991.
24. Taber, L.A. On a nonlinear theory for muscle shells: Part II—Application to the beating left ventricle. Trans. of the ASME 113:63–67; 1991.
25. Timoshenko, S.P.; Goodier, J.N. Theory of elasticity. Tokyo: McGraw-Hill/Kogakusha Ltd; 1970.
26. Tozeren, A. A static analysis of the left ventricle. ASME J. Biomech. Eng. 105:39–46; 1983.
27. Waldman, L.K.; Fung, Y.C.; Covell, J.W. Transmural myocardial deformation in the canine left ventricle: normal in vivo three dimensional finite strains. Circ. Res. 57:152–163; 1985.
28. Waldman, L.K.; Nosan, D.; Villarreal, F.; Covell, J.W. Relation between transmural deformation and local myofiber direction in canine left ventricle. Circ. Res. 63:550–562; 1988.
29. Wong, A.Y.K.; Rautaharju, P.M. Stress distribution within the left ventricular wall approximated as a thick ellipsoidal shell. Am. Heart J. 75:649–662; 1968.
30. Zerhouni, E.A.; Parish, D.M.; Rogers, W.J.; Yang, A.; Shapiro, E.P. Human heart: Tagging with MR imaging—a method for non-invasive assessment of myocardial motion. Radiology 169:59–63; 1988.

NOMENCLATURE

G = the shear modulus of elasticity
M_t = twisting moment
M_R = the moment produced by a layer of fiber located at radius R from the long axis
r = radial coordinate
Z = longitudinal coordinate
Z' = longitudinal distance from the LV base
Z_0 = longitudinal distance of the geometrical apex from the LV base
α = cone angle of the epicardium
β = cone angle of the endocardium
γ = inclination angle of the fibers within a given layer
Φ = the stress function
ψ = angle of twist
ρ = correlation coefficient (in Table 1)
σ_f = stress within a myocardial fiber
θ = angular coordinate

APPENDIX A:

FIBER ORIENTATION, AND THE TRANSMURAL TWIST GRADIENT IN A CYLINDRICAL MODEL

Moments that cause the LV to twist are generated as a result of the helical structure of the myocardial fibers. As suggested by Streeter *et al.* (22) the angle of incli-

nation, γ, of the fibers varies transmurally from about $+60°$ in the epicardium to about $-60°$ at the endocardium. Following the approach presented by Arts *et al.* (2), and using a cylindrical geometry as depicted in Fig. A1, the moment M_R applied by a layer of fibers with an inclination angle γ, located at radius r (Fig. A1) from the cylinder's axis, is given by:

$$M_R = r \cdot 2\pi r\, dr \cdot \sigma_f \cdot \sin\gamma \cdot \cos\gamma = \pi r^2\, dr \cdot \sigma_f \cdot \sin(2\gamma) \ , \qquad \text{(A1)}$$

where σ_f is the fiber's stress, assumed uniform within each layer.

Inspection of Eq. A1 indicates that the term of the right side can be viewed as a multiplication of three components: (a) a geometrical component ($\pi r^2\, dr$); (b) a fiber directional component [$\sin(2\gamma$]; and (c) a fiber stress component (σ_f). Though the third component is not entirely independent of the other two, we would like to study the contribution of each one separately.

Considering the geometrical component, it is clear that M_R increases as the square of the radius. Hence, as one moves from the endocardium to the epicardium, M_R is expected to increase substantially. Furthermore, due to the LV wall thickening, the endocardial radius decreases during systole much more than the epicardial one. It follows from these geometrical considerations that the moments generated by the epicardium decrease less than the endocardial moments during the LV contraction and myocardial thickening from the beginning to end ejection.

Considering the directional component, we can roughly divide the myocardium into three major layers: subendocardium, midwall, and subepicardium. Since most of the fibers in the midwall layer are oriented circumferentially (i.e., $\gamma \approx 0°$), the contribution of this layer to twist may be considered negligible. On the other hand, both endocardial and epicardial layers have, in absolute terms, approximately the same (but with opposite signs!) angles of inclination of the fibers. Thus, the fiber stress is expected to be similar in both layers, except for the change in sign; that is, the corresponding endocardial and epicardial moments will counteract each other.

Let us now assume that the LV contracts slightly from its ED state without any torsional deformation. It can be easily shown that as a result of wall thickening, the endocardial shortening will markedly exceed the epicardial shortening. Assume, too,

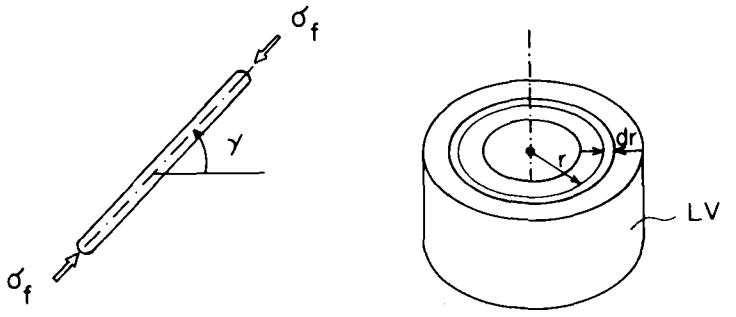

FIGURE A1. A cylindrical approximation of the LV and the corresponding representation of its fibers in a given myocardial layer.

that the sarcomere lengths (SL) at ED are about the same at both sublayers, and that the fibers' stress is, approximately, reduced linearly as the fiber shortens. Under these conditions (and without twist), it can be expected that the fibers' stress, σ_f, at the end of the contraction step in the epicardium is larger than in the endocardium.

The above analysis illuminates the inadequacy of "fibrous" cylindrical models to explain the twist phenomena. As seen, the cylindrical analysis indicates that the twist moments of the epicardium are larger than, and opposite to, the endocardial twist moments; the net result is a global twist deformation in the direction of the epicardial moments. This conclusion is valid for nonlinear material properties, as well as in the presence of myocardial anisotropy. Consequently, the endocardial layers are pulled by the epicardial layers, manifested by the epicardial twist being larger than the "dragged" endocardial twist. Clearly this description contradicts the experimental observation that the endocardial twist is larger than the epicardial twist.

APPENDIX B:

ASSESSMENT OF THE ERROR RESULTING FROM USING SMALL STRAINS ANALYSIS

The present study employs a "small strain" analysis for calculating the twist angle. However, as the measured deformations are not infinitesimal; some error is introduced in the computation. To assess the magnitude of this error, a "finite strain" analysis (e.g., see Malvern (16)) was applied to the endocardial and epicardial regions and the corresponding shear strain in the $r - \theta$ plane ($E_{r\theta}$) was calculated. The calculation was carried out using the average measured dimensions and angles of twist. The results obtained were compared to the same shear strains calculated using small strain analysis ($\varepsilon_{\rho\theta}$) and the corresponding errors were calculated as shown below. The results are outlined in Table B1. As can be observed, the small strain analysis yields an underestimation of -9.7% at the LV base and of -13.9% at the apex in the endocardial region (average = -12%). On the other hand, it yields an overestimation of 5.6% at the base and of 1.4% at the apex (average = $+4.1\%$) in the epicardium. This magnitude of error is within the range estimated by Waldman *et al.* (27) and is quite acceptable considering the large scatter of the experimental data.

TABLE B1. Estimation of the corresponding error resulting from the implementation of "small strain" analysis as compared to results obtained by "finite strains" analysis.

	Endocardium			Epicardium		
Slice	$\varepsilon_{r\theta}$	$E_{r\theta}$	Error	$e_{r\theta}$	$E_{r\theta}$	Error
Base 1	0.0418	0.0463	−9.7%	0.0266	0.0252	5.6%
2	0.0559	0.0631	−11.4%	0.0320	0.0304	5.3%
3	0.0907	0.1042	−13.0%	0.0499	0.0480	4.0%
Apex 4	0.1130	0.1312	−13.9%	0.0627	0.0618	1.4%

$\varepsilon_{r\theta}$ = the shear strain calculated using "small strains" analysis; $E_{r\theta}$ = the shear strain calculated using "finite strains" analysis; Error $\triangleq 100\%\ (\varepsilon_{r\theta} - E_{r\theta})/E_{r\theta}$.

Calculations were carried out for the shear strain in the $r\theta$ plane.